Supplementary Material for PCCP

Resistive Memories Based on Rose Bengal and Related Xanthene Derivatives: Insights from Modeling Charge Transport Properties

Daniele Fazzi[†*], Chiara Castiglioni[†#] and Fabrizia Negri[‡*]

[†]Politecnico di Milano, Dipartimento di Chimica, Materiali e Ing. Chimica "G. Natta", p.za Leonardo da Vinci 32, 20133 Milano, Italy, and INSTM, UdR Milano.

[‡]Università degli Studi di Bologna, Dipartimento di Chimica "G. Ciamician", via F. Selmi 2, 40126 Bologna Italy and INSTM, UdR Bologna.

E-mail: daniele.fazzi@mail.polimi.it, fabrizia.negri@unibo.it

CORRESPONDING AUTHOR daniele.fazzi@mail.polimi.it, fabrizia.negri@unibo.it

1. Mulliken charge distribution on the molecular backbone

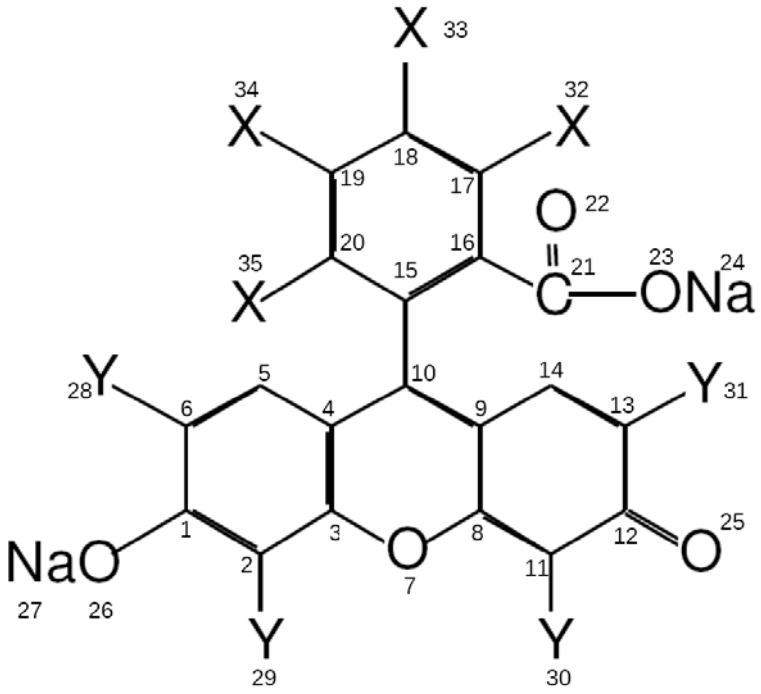

Figure S1. Xanthene-based chemical structure with atom numbers.

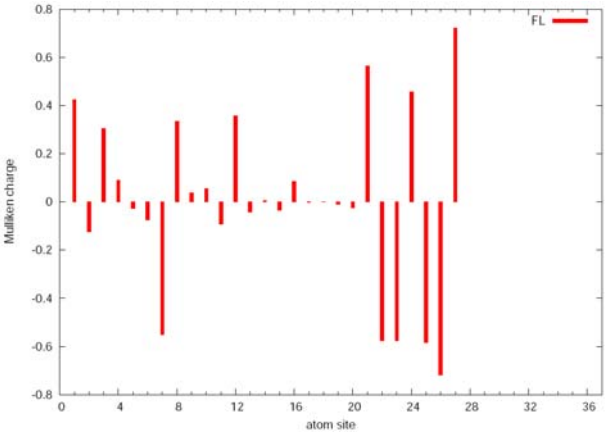

Fluorescein (FL)

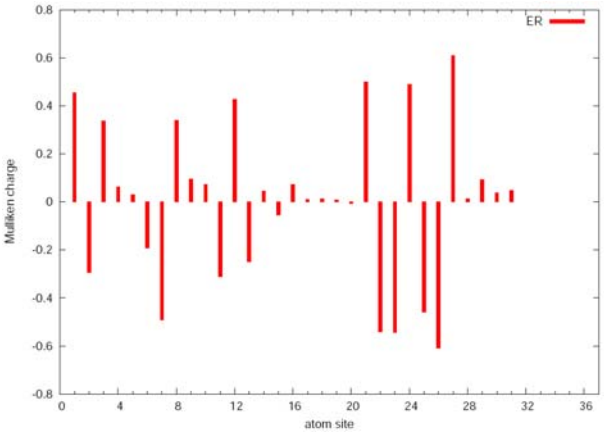

Erythrosin B (ER)

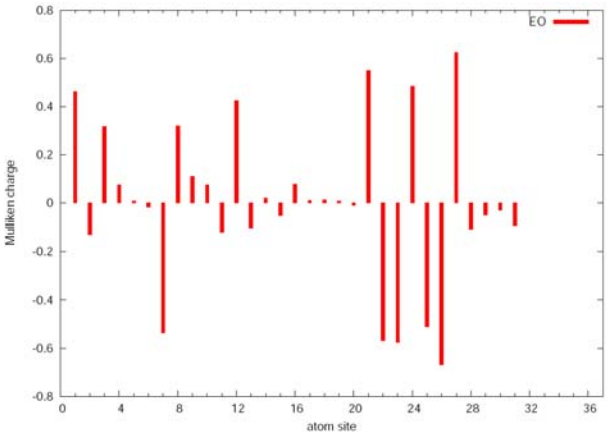

Eosyn Y (EO)

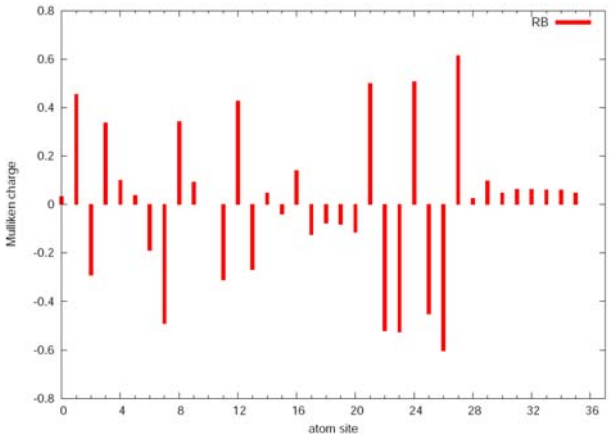

Rose Bengal (RB)

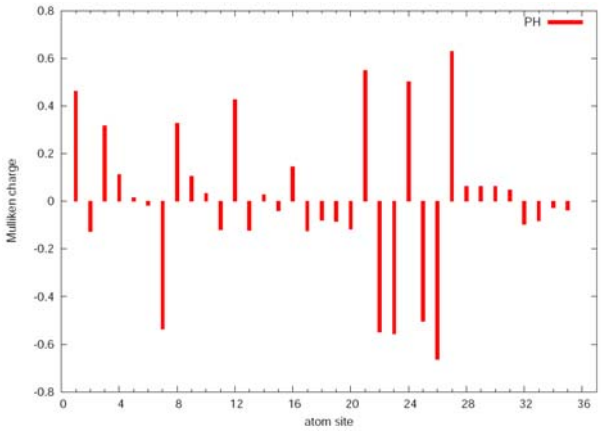

Phloxine B (PH)

Figure S1.1 . Mulliken charge distribution (B3LYP/6-31G**, 3-21G** for I atoms) in the neutral state of the Xanthene derivatives investigated. From top to bottom: from Fluorescein (FL) to Phloxine B (PH). Atom numbering as defined in Figure S2.

2. C-Y neutral

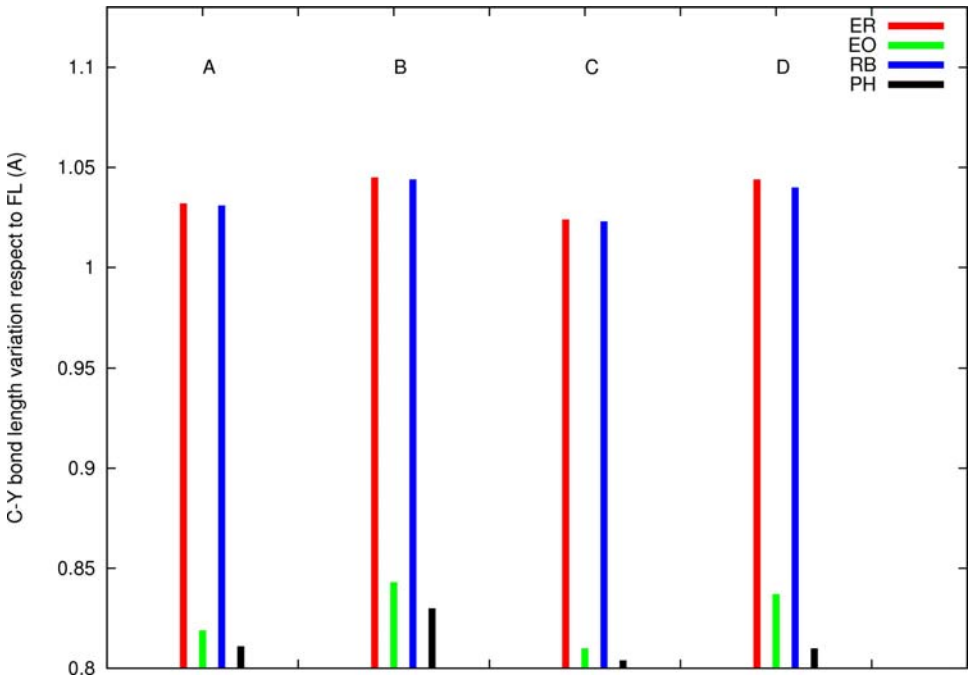

Figure S2. C-Y bond length variations with respect to the FL compound. B3LYP/6-31G**, 3-21G** basis set for iodine (neutral state) .

3. One-electron energy levels of the neutral species.

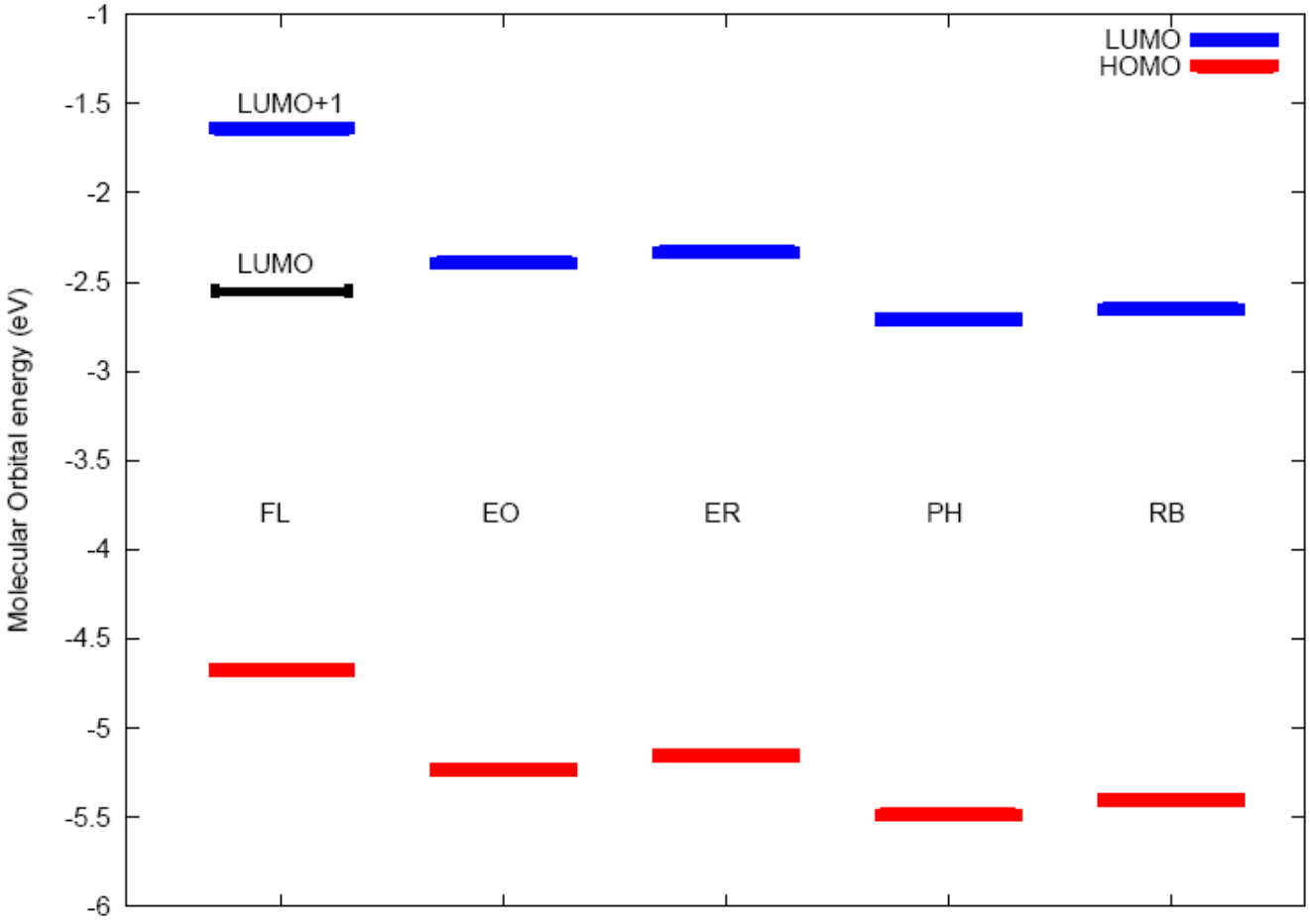

Figure S3. Frontier molecular orbital energy levels calculated at the B3LYP/6-31G** (3-21G** for iodine atoms) level (HOMO -red line- and LUMO -blue line-) for each xanthene derivative. The LUMO+1 level of FL correlates with the LUMO levels of EO, ER, PH and RB.

4. Molecular orbital shapes of the reduced species.

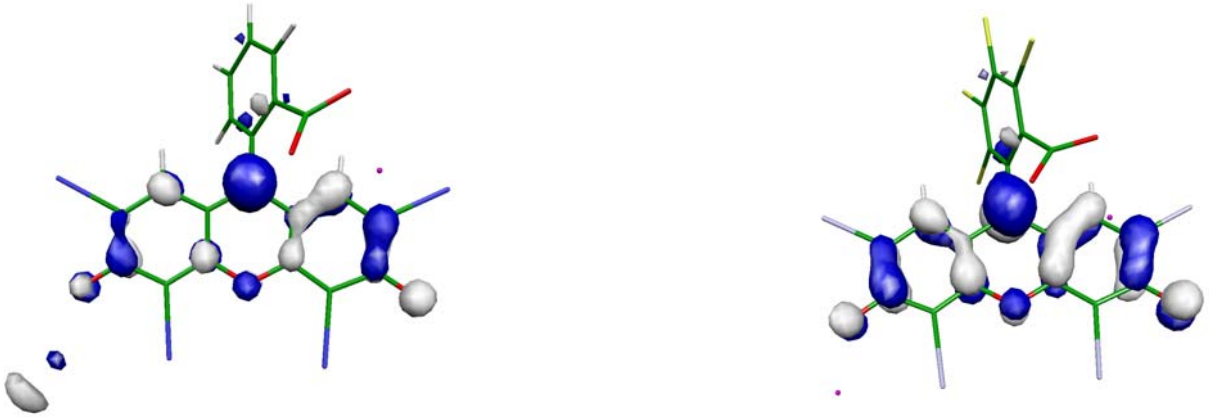

ER: SOMOα RB: SOMOα

Figure S4. Singly occupied molecular orbital (SOMOα) of ER and RB mono-reduced species.

5. Bond length variation of C-Y bonds upon reduction.

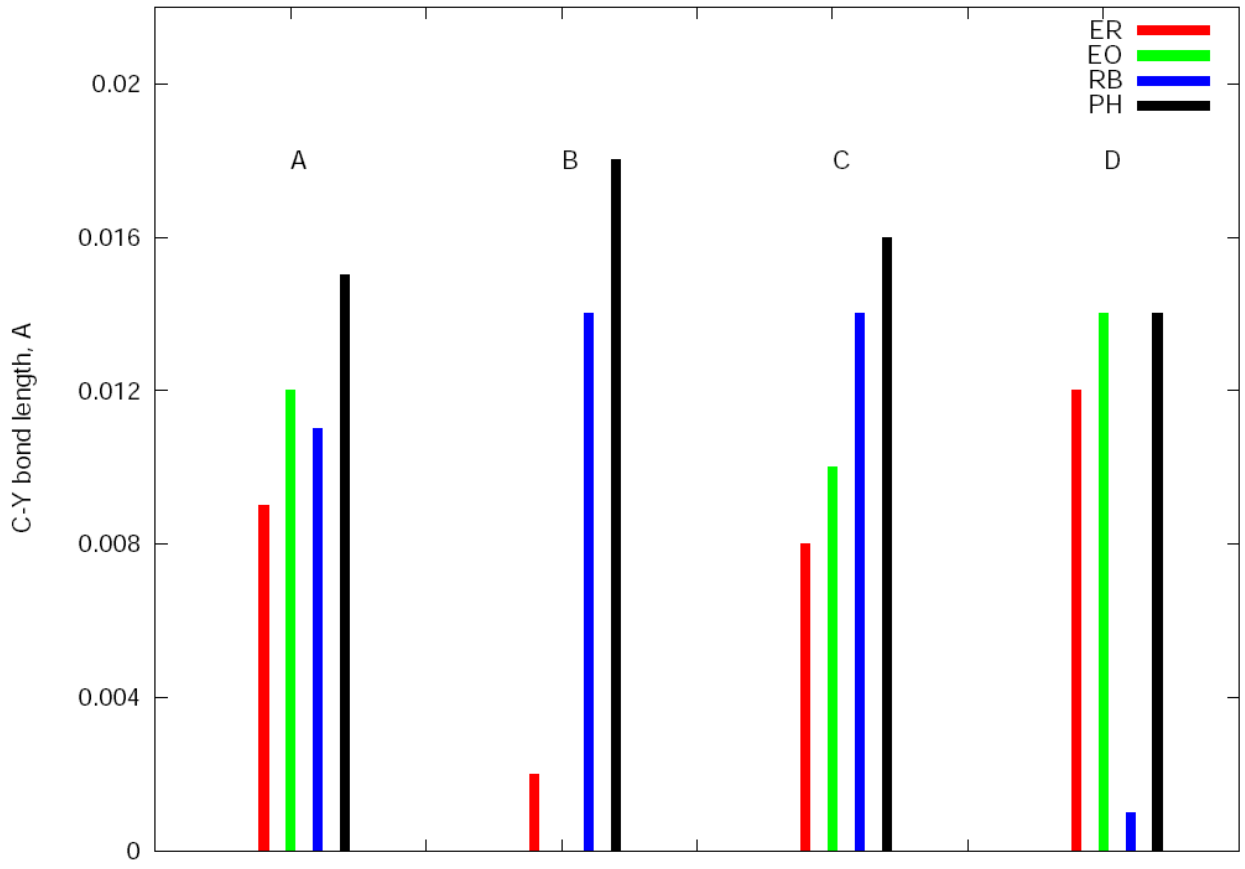

Figure S5 C-Y bond-length variation upon the reduction process (B3LYP/6-31G**, 3-21G** for I atoms)

6. Contributions of vibrational frequencies to the intramolecular reorganization energy, as computed from HR parameters (S_j).

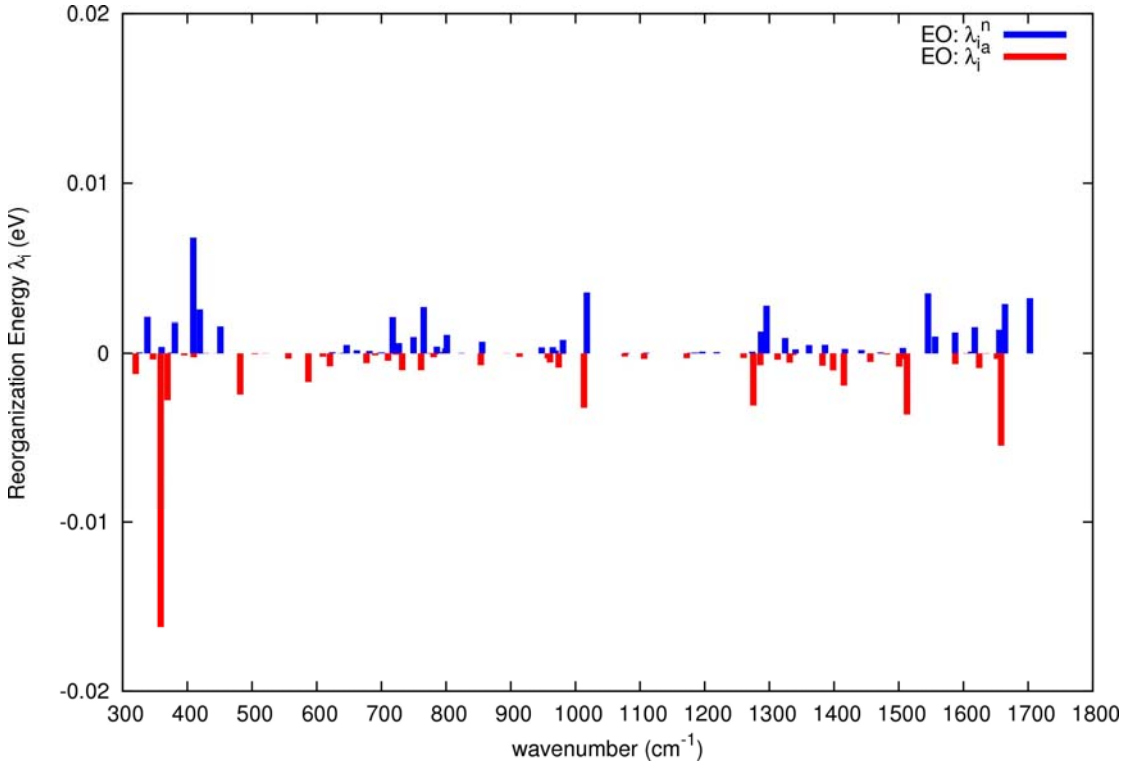

Figure S6.1. Contributions of each vibrational frequency to the intramolecular reorganization parameters, as resulting from the computation of the HR parameters for the EO compound. (top, blue) neutral state; (bottom, red) anionic state. B3LYP/6-31G**.

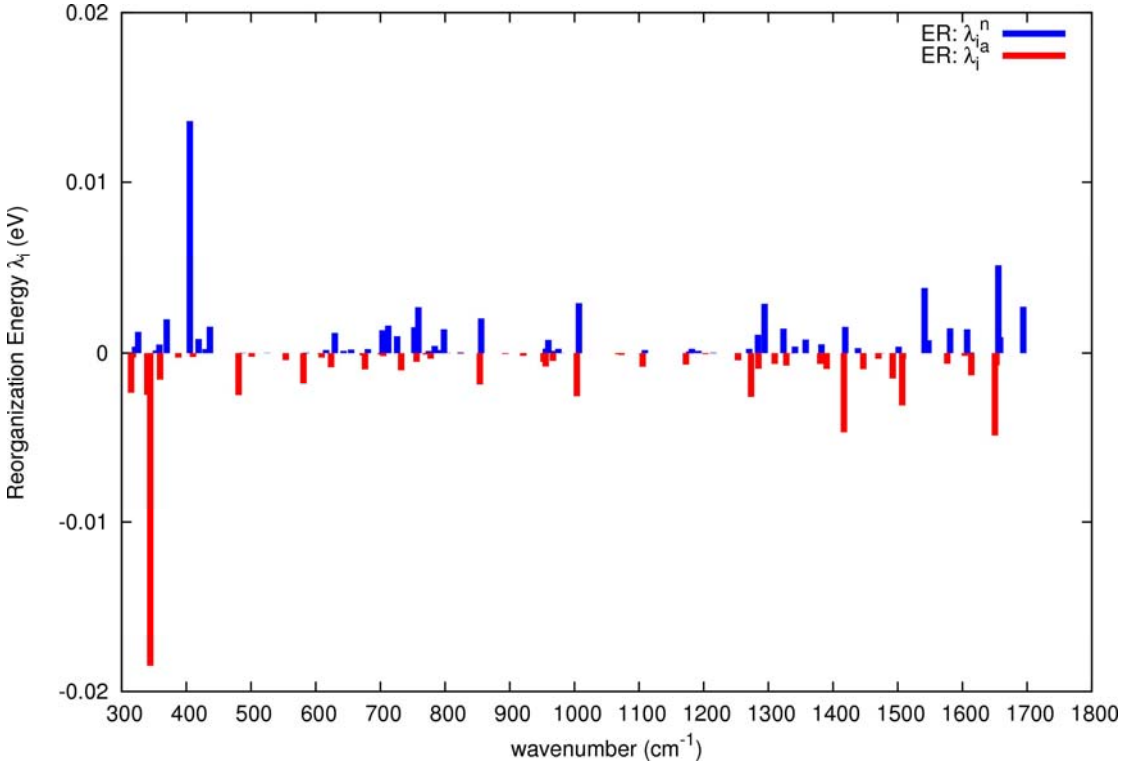

Figure S6.2. Contributions of each vibrational frequency to the intramolecular reorganization parameters, as resulting from the computation of the HR parameters for the ER compound. (top, blue) neutral state; (bottom, red) anionic state. B3LYP/6-31G**, 3-21G** for iodine.

7. Calculated electron transfer integrals V_{ij} (B3LYP/6-31G, 3-21G** for iodine) as a function of the displacement along the xanthene moiety.**

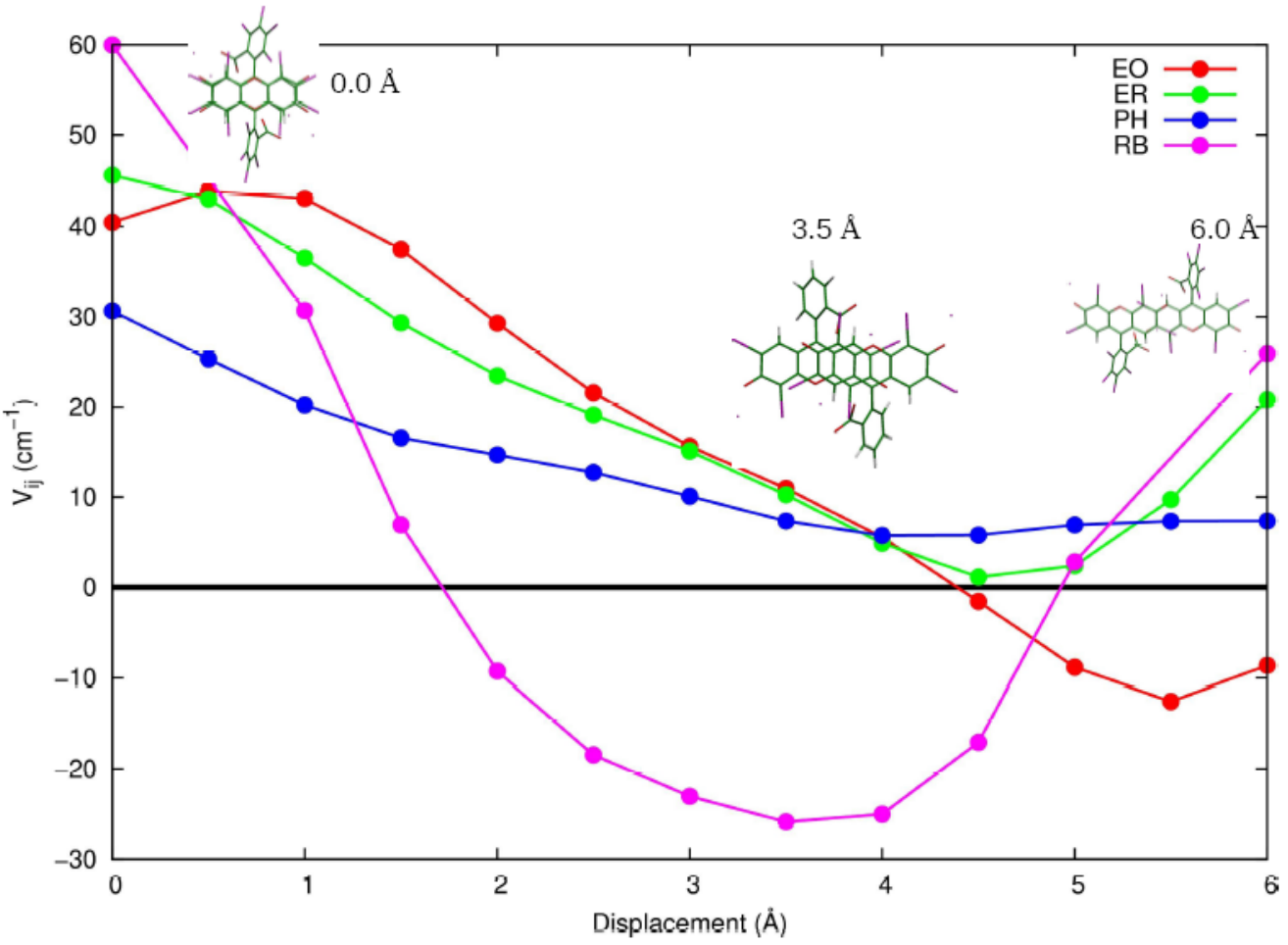

Figure S7. Computed charge transfer intergrals V_{ij} for two cofacial molecules as a function of the translation along the long axis of the xanthene moieties. The sketches of the molecules (RB) forming the dimer are reported for selected translations. While the V_{ij} dependence against short axis translation shows a clear trend across the four compounds, the dependence against the long axis translation is less clear partly because of the lare separation between molecules in the dimmer, partly because of the different bond lengths and out of plane deformation of the xanthene moiety in the four derivatives. These differences prevent a strict comparison among the curves in the Figure.

8. Absolute computed energies for the four systems investigated (for the meaning of the critical point, i.e. $E_n^{geo\text{-}n}$, $E_n^{geo\text{-}a}$, $E_a^{geo\text{-}a}$ and $E_a^{geo\text{-}n}$ see Figure 2 in the article) **and reorganization energy calculated by using the Adiabatic Potential (AP) approach**

	EO	ER	PH	RB
$E_n^{geo\text{-}n}$ (Hartree)	-11753.430714	-29026.903425	-13591.774729	-30865.234503
$E_n^{geo\text{-}a}$ (Hartree)	-11753.426604	-29026.898981	-13591.765874	-30865.223924
$E_a^{geo\text{-}a}$ (Hartree)	-11753.484872	-29026.956327	-13591.480091	-30865.299681
$E_a^{geo\text{-}n}$ (Hartree)	-11753.480959	-29026.952073	-13591.833742	-30865.292251
λ_i (eV)	0.22	0.24	0.41	0.49